This is a preprint of an article published in Plant Journal. The final authenticated version is available online at: https://doi.org/10.1111/tpj.15468

Vessel- and ray-specific monolignol biosynthesis as an approach to engineer fiber-hypolignification and enhanced saccharification in poplar

Barbara De Meester[a,b], Ruben Vanholme[a,b], Lisanne de Vries[a,b], Marlies Wouters[a,b], Jan Van Doorsselaere[c] and Wout Boerjan[a,b,*]

[a]Department of Plant Biotechnology and Bioinformatics, Ghent University, Technologiepark 71, 9052 Ghent, Belgium

[b]VIB Center for Plant Systems Biology, Technologiepark 71, 9052 Ghent, Belgium

[c]Higher Institute for Nursing and Biotechnology, VIVES University College, Wilgenstraat 32, 8800 Roeselare, Belgium

[*]Correspondence (Tel. +32 9 331 38 81; fax +32 9 331 38 09; email wout.boerjan@psb.vib-ugent.be)

ORCID IDs: 0000-0003-2485-330X (B.D.M.); 0000-0002-3245-9081 (L.d.V.); 0000-0003-2254-0051 (M.W.); 0000-0001-5848-3138 (R.V.); 0000-0003-1495-510X (W.B.)

CORRESPONDING AUTHOR:

Wout Boerjan

Center for Plant Systems Biology

VIB - Ghent University

Technologiepark 71

B-9052 Gent (Belgium)

KEY WORDS: lignin, lignin engineering, lignin modification-induced dwarfism, good neighbors for lignification, *Populus tremula* x *P. alba*, fiber hypolignification, saccharification, *ProSNBE*, CRISPR/Cas9, CCR.

SIGNIFICANCE STATEMENT:

Lowering lignin amount makes woody plants more amenable to processing into fermentable sugars, but typically also results in growth defects. By reintroducing lignin biosynthesis specifically into vessels and rays, the dwarfed phenotype of low-lignin *ccr2* poplars was restored. As we found that monolignols can also travel between the different cell types in poplar wood, the anticipated fiber-hypolignification and increased processing efficiency was achieved by limiting the supply of monolignols made by vessels and rays.

SUMMARY

Lignin is one of the main factors determining recalcitrance to processing of lignocellulosic biomass towards bio-based materials and fuels. Consequently, wood of plants engineered for low lignin content is typically more amenable to processing. However, lignin-modified plants often exhibit collapsed vessels and associated growth defects. Vessel-specific reintroduction of lignin biosynthesis in dwarfed low-lignin *cinnamoyl-CoA reductase1* (*ccr1*) Arabidopsis mutants using the *ProSNBE:AtCCR1* construct overcame the yield penalty while maintaining high saccharification yields and showed that monolignols can be transported between the different xylem cells acting as 'good neighbors' in Arabidopsis. Here, we translated this research into the bio-energy crop poplar. By expressing *ProSNBE:AtCCR1* into CRISPR/Cas9-generated *ccr2* poplars, we aimed for vessel-specific lignin biosynthesis to (i) achieve growth restoration while maintaining high saccharification yields and (ii) study the existence of 'good neighbors' in poplar wood. Analyzing the resulting *ccr2 ProSNBE:AtCCR1* poplars showed that vessels and rays act as good neighbors for lignification in poplar. If sufficient monolignols are produced by these cells, monolignols migrate over multiple cell layers, resulting in a restoration of the lignin amount to wild-type levels. If the supply of monolignols is limited, the monolignols are incorporated into the cell walls of the vessels and rays producing them and their adjoining cells resulting in fiber hypolignification. One such fiber-hypolignified line had 18% less lignin and, despite its small yield penalty, had an increase of up to 71% in sugar release on a plant base upon saccharification.

INTRODUCTION

Today's fossil-based economy results in a net increase of CO_2 in the Earth's atmosphere, and is thereby a major cause of global climate change. To counter this, a shift towards a bio-based, carbon-negative economy is highly needed (Vanholme et al., 2013a). Lignocellulosic biomass can play a crucial role in such a bio-based economy by serving as a feedstock for the production of both energy and a plethora of chemicals (Vanholme et al., 2013a; Linger et al., 2014; Marriott et al., 2016; Rinaldi et al., 2016; Schutyser et al., 2018). Lignocellulosic biomass mainly consists of cellulosic and hemicellulosic polysaccharides embedded in lignin. In the enzymatic hydrolysis-based biorefinery process, the cell wall polysaccharides are depolymerized into monomeric sugars through an enzymatic process called saccharification (Mariott et al., 2016). These sugar monomers can be converted into bioethanol or other bio-based products through fermentation by microorganisms.

Lignin is an aromatic heteropolymer that provides strength and hydrophobicity to the plant cell wall. Lignin in dicotyledonous plants is generally derived from the monolignols coniferyl and sinapyl alcohol and low levels of *p*-coumaryl alcohol (Vanholme et al., 2019). Depending on the plant species, other phenolic metabolites also act as monomers for lignification. In dicotyledonous plants, the lignin monomers are synthesized via the general phenylpropanoid- and monolignol-specific pathways starting from the amino acid phenylalanine (Vanholme et al., 2019). After their biosynthesis in the cytoplasm, the lignin monomers are translocated to the cell wall (Perkins et al., 2019; Vermaas et al., 2019). There, the monomers are oxidized by peroxidases and/or laccases for subsequent polymerization into the lignin polymer through radical coupling (Wang et al., 2013; Tobimatsu and Schuetz, 2019). Upon incorporation into the polymer, the monolignols coniferyl, sinapyl, and *p*-coumaryl alcohol produce guaiacyl (G), syringyl (S), and *p*-hydroxyphenyl (H) units, respectively.

Despite the use of lignocellulosic biomass as a renewable resource has enormous potential, the reality of a cost-competitive lignocellulosic biorefinery involves overcoming several obstacles such as the high enzyme cost and the biomass recalcitrance towards saccharification (Silva et al., 2018). Up to now, enzymatic saccharification making use of cellulases is the most effective, convenient, viable and eco-friendly approach for lignocellulosic biomass hydrolysis (Chandel et al., 2018). These cellulase enzymes are largely produced from fungal species such as

Trichoderma sp. In spite of substantial (biotechnological) research carried out on these enzymes, it is estimated that the cellulolytic enzymes still represent around a quarter of the total cost of generating cellulosic ethanol (Klein-Marcuschamer et al., 2012; Silva et al., 2018). Furthermore, the accessibility of the cell wall polysaccharides for enzymatic hydrolysis is hampered because of the natural recalcitrance of plant cell walls, largely caused by the presence of lignin (Mahon and Mansfield, 2019). To improve this accessibility, the lignocellulosic matrix can be loosened via physicochemical pretreatments (Vanholme et al., 2013a; Maurya et al., 2015). There are many different lignocellulosic biomass pretreatments, each increasing the lignocellulose accessibility/digestibility in very different ways. However, up to now, the conventional pretreatment techniques are cost-intensive because of the immoderate usage of energy (e.g. high temperatures) and chemicals (Chandel et al., 2018). Moreover, post-pretreatment operations such as disposing by-products and treatment of solid and liquid waste further increase the expenses. Lignocellulosic biomass with reduced cell wall recalcitrance would help reducing the operational costs of lignocellulosic biorefineries. To this end, plants can be engineered to deposit less lignin or produce lignin polymers that are more amenable to deconstruction (Chen and Dixon, 2007; Van Acker et al., 2013; Vanholme et al., 2013b; Mottiar et al., 2016; Chanoca et al., 2019; Oyarce et al., 2019). However, lignin-modified plants that show the highest improvement in saccharification efficiency typically suffer from growth perturbations (Bonawitz and Chapple, 2013; Van Acker et al., 2013; Vanholme et al., 2013b; Muro-Villanueva et al., 2019; Ha et al., 2021). For example, transgenic poplars downregulated for *CINNAMOYL-CoA REDUCTASE2* (*CCR2*) had an up to 24% reduction in lignin amount and an up to 140% increased saccharification efficiency (Leplé et al., 2007; Van Acker et al., 2014). Unfortunately, these poplars had a significantly reduced biomass yield offsetting their gains in saccharification yield. Moreover, the downregulation of *CCR2* via RNAi in poplar appeared to be unstable as judged by the patchy appearance of the red xylem phenotype associated with reduced CCR activity (Van Acker et al., 2014). By contrast, the knock-out of *CCR2* in poplar, generated by CRISPR/Cas9, resulted in a uniformly distributed red xylem phenotype (De Meester et al., 2020). These stable *ccr2* knock-out poplars had a severely reduced lignin amount, but were extremely dwarfed.

The mechanisms underlying this lignin modification-induced dwarfism (LMID) are still poorly understood, but several causes have been postulated to explain this

phenomenon (Bonawitz and Chapple, 2013; Muro-Villanueva et al., 2019). A first potential cause of LMID is the lack or the hyperaccumulation of pathway intermediates or derivates, such as cinnamic acid (hyperaccumulation in *ref3-2* mutants; Schilmiller et al., 2009) or salicylic acid (hyperaccumulation in HCT-deficient plants; Gallego-Giraldo et al., 2011). A second potential cause of LMID is that the cell wall integrity system senses defects in the cell wall and consequently activates a cascade of transcriptional changes to overcome these cell-wall defects, but this reallocation of resources might come at the expense of plant growth. The role of transcriptional changes in LMID has been demonstrated by the (partial) restoration of biomass yield upon mutation of subunits of the transcriptional coregulator Mediator in *ref8-1* mutants (Bonawitz et al., 2014). The third and most prominent cause of LMID is the collapse of vessels due to their weakened cell walls, which, in turn, results in the inability of the plant to efficiently transport nutrients and water from the roots to the aerial parts (Yang et al., 2013; Vargas et al., 2016; De Meester et al., 2018). For example, both *CCR2*-downregulated and *ccr2* knock-out poplars displayed collapsed vessels and associated yield penalties (Leplé et al., 2007; De Meester et al., 2020). To overcome this vessel collapse, lignin biosynthesis has been specifically reintroduced in the vessels of low-lignin mutants. In two independent studies, *VASCULAR-RELATED NAC DOMAIN 6* (*VND6*) and *VND7* promoter sequences were used to drive the expression of either *CINNAMATE 4-HYDROXYLASE* (*C4H*) or *CAFFEOYL SHIKIMATE ESTERASE* (*CSE*) in the *c4h* and *cse* Arabidopsis mutants, respectively (Yang et al., 2013; Vargas et al., 2016). Although this strategy largely restored vessel shape and plant biomass, these promoter sequences were not strong and/or specific enough to fully overcome the biomass yield penalty, and at the same time maintain the high saccharification efficiency of the respective low-lignin mutants. In contrast, *ProSNBE*, an artificial promoter consisting of three tandem repeats of the *cis*-regulatory *SECONDARY WALL NAC BINDING ELEMENT* (*SNBE*) of the Arabidopsis *XYLEM CYSTEINE PROTEASE1* (*XCP1*) promoter, conferred strong and vessel-specific expression in Arabidopsis (Zhong et al., 2010; McCarthy et al., 2011). When using *ProSNBE* to drive the expression of the Arabidopsis *CINNAMOYL-COA REDUCTASE1* (*AtCCR1*) in an Arabidopsis *ccr1* mutant background, the total plant biomass was fully restored, while maintaining the high saccharification efficiency of the original *ccr1* mutants (De Meester et al., 2018). On a plant basis, these *ccr1 ProSNBE:AtCCR1* lines had a fourfold increase in sugar release when compared to

the wild type, making them the Arabidopsis lines with the highest improvement in saccharification yield reported so far.

Despite their vessel-specific monolignol biosynthesis, *ccr1 ProSNBE:AtCCR1* Arabidopsis plants showed (partial) restoration of lignification and cell wall integrity in both vessels and xylary fibers (De Meester et al., 2018). This observation showed that monolignols synthesized in the vessel cells not only lignify the vessel cell wall but also contribute to the lignification of the cell walls of neighboring (xylary fiber) cells. The existence of so-called 'good neighbors for lignification' was proposed based on the observation of *postmortem* lignification of tracheary elements in *Zinnia elegans* and *Arabidopsis* cell cultures (Hosokawa et al., 2001; Tokunaga et al., 2005; Pesquet et al., 2013). In Arabidopsis, in addition to transport of monolignols from vessels to xylary fibers, also transport from non-lignifying parenchyma cells to vessels and xylary fibers, and from xylary fibers to vessels has been observed (Smith et al., 2013; Smith et al., 2017; De Meester et al., 2018). In poplar, the migration of monomers into the cell wall of adjoining cells has been suggested by the observation that the lignin composition of fiber walls adjoining vessel cells resembles more that of vessel walls than that of fiber walls in fiber-rich areas (Gorzsás et al., 2011). However, it cannot be excluded that these differences in cell wall composition are merely the consequence of differences in gene expression.

Here, *ProSNBE* was used to drive the expression of the Arabidopsis (At) *CCR1* gene in dwarfed *ccr2* knock-out poplars. By aiming for vessel-specific lignin biosynthesis in poplar, we wanted to investigate (i) whether this approach allows to restore vessel integrity and biomass yield of CRISPR/Cas9-generated *ccr2* knock-out poplars while maintaining fiber hypolignification and improved saccharification efficiency, (ii) if vessel cells also act as good neighbors for lignification in poplar and, if they do, (iii) to what extent monolignols can migrate into the xylary fiber cell layers.

RESULTS

ProSNBE confers expression in vessels and rays of poplar

We aimed for vessel-specific expression of *AtCCR1* in *ccr2* knock-out mutant poplar as a strategy to restore plant growth. To achieve this, a promoter was required that specifically drives *AtCCR1* expression in the vessels, and not in the fibers, of poplar. *ProSNBE* was shown to direct expression specifically in the vessels of Arabidopsis (De Meester et al., 2018). In order to investigate the expression pattern

conferred by *ProSNBE* in poplar, the previously described *ProSNBE*:*β-GLUCURONIDASE* (*GUS*) construct (De Meester et al., 2018) was used to transform poplar. A total of sixteen transgenic *ProSNBE:GUS* lines were grown in soil and sections through developing stems of 5-month-old trees were analyzed. All trees displayed *GUS* expression in the vessel and ray cells (Figure S1). GUS staining in the ray cells was predominantly present in contact rays, which make direct connections with adjacent vessel elements through pits. These pits play an important role during xylem cell differentiation, providing channels for the transfer of wall precursors (such as monolignols), metabolites and signals that control differentiation (Murakami et al., 1999; Larisch et al., 2012). Although *ProSNBE* directs expression not solely to the vessels, but also to the rays of poplar, it does not confer expression in fibers. Therefore, it was used for the envisioned complementation approach.

Selection of *ccr2 ProSNBE:AtCCR1* lines for further analysis

In an attempt to restore vessel integrity and growth of dwarfed *ccr2* poplars (Figure S2) (De Meester et al., 2020), *ProSNBE* was used to drive the expression of the Arabidopsis *CCR1* gene in the *ccr2* poplar background. We therefore designed a construct harboring both the *ProSNBE:AtCCR1* transgene and the coding sequences of *Cas9* and gRNA1 previously used to generate *ccr2* mutant poplars (De Meester et al., 2020). After cloning into the *p201N-Cas9* vector, the resulting vector was used for *Agrobacterium*-mediated transformation of poplar. In total, 24 transgenic plantlets were generated. Sequencing the PCR-amplified region targeted by gRNA1 showed that nine plantlets contained more than two different *CCR2* sequences. These chimeric lines were not analyzed further. The remaining fifteen plantlets carried biallelic mutations in *CCR2* and were grown, together with wild-type controls, in the greenhouse for five months (Table S1, Figure S3). In contrast to the severely dwarfed *ccr2* knock-outs, no substantial differences in growth between the *ccr2 ProSNBE:AtCCR1* lines and wild type were observed. After harvesting, the stems were dried and debarked. A selection of these lines for further analysis was made based on screening for the sugar release upon saccharification without pretreatment of cell-wall prepped stem material. Note that this screening was done on the first stem harvest of each transformed line and hence, only one plant per line was analyzed. Based on this analysis, *ccr2 ProSNBE:AtCCR1* lines 3, 10 and 18 had the highest sugar yield upon saccharification (Table S1). Of these, *ccr2 ProSNBE:AtCCR1* lines 3 and 10 had a normal xylem

coloration. By contrast, *ccr2 ProSNBE:AtCCR1* line 18, the line which had the highest sugar yield upon saccharification, was the only line to exhibit a reddish xylem coloration. These three *ccr2 ProSNBE:AtCCR1* lines were chosen for further analysis.

The introduction of *ProSNBE:AtCCR1* (partially) restores plant height of *ccr2* mutant poplar

The three selected *ccr2 ProSNBE:AtCCR1* lines were clonally propagated to obtain multiple biological replicates for further analysis. The biological replicates, together with wild-type controls, were grown for five months in the greenhouse. Plant height was measured monthly. The *ccr2 ProSNBE:AtCCR1* lines 3 and 10 showed no difference in plant height as compared to the wild type (Figure 1a, b; Table 1). In contrast, after four months of growth in the greenhouse, *ccr2 ProSNBE:AtCCR1* line 18 started to show a reduction in plant height when compared to the wild type. After growing for five months, *ccr2 ProSNBE:AtCCR1* line 18 had a height reduction of 12% when compared to the wild-type control (Figure 1a, b; Table 1). In line with the height data, the fresh stem weight (with and without bark) and dry stem weight of *ccr2 ProSNBE:AtCCR1* lines 3 and 10 were not significantly different from those of the wild-type control, whereas *ccr2 ProSNBE:AtCCR1* line 18 showed a tendency to have a reduced weight as compared to the wild-type control (Table 1). However, the biomass yield reduction of *ccr2 ProSNBE:AtCCR1* line 18 remained relatively small when compared to the severe yield penalty of *ccr2* knock-out poplars (Figure S2; De Meester et al., 2020).

The color of the xylem of the three *ccr2 ProSNBE:AtCCR1* lines was evaluated on both cross-sections and debarked stems; *ccr2 ProSNBE:AtCCR1* lines 3 and 10 displayed a white-to-beige coloration of the xylem, similar to that of the wild type (Figure 1c). By contrast, *ccr2 ProSNBE:AtCCR1* line 18 had a red coloration of the xylem that was uniformly distributed along the stem (Figure 1c).

Microscopic analysis of *ccr2 ProSNBE:AtCCR1* poplar stems reveals the existence of good neighbors for lignification in poplar

Based on reporter gene analysis, *ProSNBE* confers expression in vessel and ray cells (Figure S1). To examine whether, and to what extent, these cells act as good neighbors for lignification in poplar, and whether the anticipated recovery of vessel integrity along with hypolignification of the fibers was achieved, the lignin deposition in

the stems of the three selected *ccr2 ProSNBE:AtCCR1* lines was visualized via Mäule staining (Figure 2).

Similarly to the wild type, *ccr2 ProSNBE:AtCCR1* lines 3 and 10 showed round, open vessels (Figure 2a). However, the uniform coloration of the xylem upon Mäule staining indicated that lignin deposition was not only (fully) recovered in vessels and rays, but also in fibers in these two *ccr2 ProSNBE:AtCCR1* lines. The intensity of the coloration suggested that the lignin deposition in *ccr2 ProSNBE:AtCCR1* lines 3 and 10 was comparable to that of the wild type.

In contrast, *ccr2 ProSNBE:AtCCR1* line 18 displayed slightly irregular vessels (Figure 2a, b). The coloration upon Mäule staining was less intense as compared to that of the wild type, indicative of a reduction in lignin amount in this transgenic line (Figure 2a). In contrast to *ccr2 ProSNBE:AtCCR1* lines 3 and 10, the (reduced) coloration upon Mäule staining was not uniformly distributed over the xylem. The cell walls of vessel and ray cells, and of fibers adjoining these cells, were stained more intensely (suggesting that these cells had a higher lignin content) than the cell walls of non-adjoining fibers located in fiber-rich areas (and thus further away from the monolignol-producing vessels and rays) (Figure 2b).

Taken together, these results show that vessels and rays act as good neighbors for lignification in poplar. In *ccr2 ProSNBE:AtCCR1* lines 3 and 10, vessels and rays produce monolignols that are not only transported and incorporated into the cell walls of the cells producing them, but also into the cell walls of adjoining and even non-adjoining fibers, thereby (seemingly) restoring lignin deposition in all xylem cells (Note S1, Figure S4 and S5). In *ccr2 ProSNBE:AtCCR1* line 18, the supply of monolignols produced by the vessels and rays is limited. In this case, monolignols are polymerized predominantly in the cell walls of the cells producing them and the adjoining fibers. Hence, in *ccr2 ProSNBE:AtCCR1* line 18, the envisioned hypolignification of the fibers was achieved together with a (partial) restoration of vessel integrity and growth.

ccr2 ProSNBE:AtCCR1 **line 18 has a relatively low** ***AtCCR1*** **expression and an altered cell wall**

Microscopic analysis of the *ccr2 ProSNBE:AtCCR1* lines suggested that the lignin amount was lower in *ccr2 ProSNBE:AtCCR1* line 18 when compared to that of *ccr2 ProSNBE:AtCCR1* lines 3 and 10 (Figure 2). In accordance, quantitative reverse transcription (RT-q)PCR showed that the relative expression level of *AtCCR1* in *ccr2*

ProSNBE:AtCCR1 line 18 was ~8-fold lower when compared to that of *ccr2 ProSNBE:AtCCR1* lines 3 and 10 (which showed no significant differences in *AtCCR1* expression level between them) (Figure 3).

To evaluate the lignocellulosic biomass composition of the three selected *ccr2 ProSNBE:AtCCR1* lines, the cell wall residue (CWR), the cellulose and matrix polysaccharide content, and the lignin content and composition of dried debarked stem material were determined (Table 2). CWR was prepared by applying a sequential extraction to remove soluble compounds from the biomass. The fraction of CWR (as % of the dry weight), the cellulose and matrix polysaccharide amount, the acetyl bromide lignin amount and thioacidolysis-based lignin composition of *ccr2 ProSNBE:AtCCR1* lines 3 and 10 were not statistically different from those of the wild type. In contrast, *ccr2 ProSNBE:AtCCR1* line 18 had 1.5% less CWR, and thus relatively more soluble compounds, than the wild type, while having an equal cellulose and matrix polysaccharide amount (as %CWR). In line with its reduced Mäule staining intensity, the acetyl bromide lignin amount of *ccr2 ProSNBE:AtCCR1* line 18 was decreased by 18% compared to that of the wild type. In addition, *ccr2 ProSNBE:AtCCR1* line 18 lignin released substantially less monomers (H+G+S), and had an increased relative abundance of H units. The S/G ratio of *ccr2 ProSNBE:AtCCR1* line 18 lignin was equal to that of wild-type lignin. Incorporation of ferulic acid, which is a known minor constituent of lignin, results in the release of three different units after thioacidolysis: FA-I and FA-II are derived from ferulic acid (or ferulate ester) starting units coupled via their *O*–4 position in β–*O*–4 interunit bonds, whereas the CCR marker (also called A_G in Ralph et al. (2008)) is derived from ferulic acid that has undergone twice a β–*O*–4 coupling at its β-position (Liu et al., 2021). In agreement with previously reported results for plants deficient in CCR (Goujon et al., 2003; Leplé et al., 2007; Mir Derikvand et al., 2008; Van Acker et al., 2014; De Meester et al., 2020), the relative abundance of all three ferulic acid units was increased in *ccr2 ProSNBE:AtCCR1* line 18 lignin (but not in *ccr2 ProSNBE:AtCCR1* line 3 and 10) when compared to wild-type lignin (Table 2).

ccr2 ProSNBE:AtCCR1 line 18 has an increased saccharification potential

Because lignin amount and composition greatly influence saccharification yield, we determined the saccharification potential of *ccr2 ProSNBE:AtCCR1* line 18 in conditions of limited saccharification (Figure 4). As a control, we included wild type and

ccr2 ProSNBE:AtCCR1 lines 3 and 10. The glucose yield per fraction of CWR was determined after either acid (1 M HCl, 80°C, 2 h), alkaline (62.5 mM NaOH, 90°C, 3 h) or no pretreatment. Independent of the pretreatment, the glucose yield of *ccr2 ProSNBE:AtCCR1* lines 3 and 10 was equal to that of the wild type, while that of *ccr2 ProSNBE:AtCCR1* line 18 was significantly higher (Figure 4a-c). More specifically, after 48 h of saccharification, the glucose yield (expressed as mass % of the CWR) of non-pretreated samples increased from 7.5% in the wild type to 17.3% in *ccr2 ProSNBE:AtCCR1* line 18 (i.e., a relative increase of 131%), after acid pretreatment from 8.3% to 19.7% (i.e., a relative increase of 137%), and after alkaline pretreatment from 20.3% to 30.1% (i.e., a relative increase of 48%). To take the yield penalty of *ccr2 ProSNBE:AtCCR1* line 18 into account, its glucose yield was expressed on a plant basis (Figure 4d). After no and acid pretreatment, *ccr2 ProSNBE:AtCCR1* line 18 had an increased sugar yield on a plant basis, with a relative increase of 65% and 71% compared to the wild type, respectively. After alkaline pretreatment, *ccr2 ProSNBE:AtCCR1* line 18 had a sugar yield on a plant basis that was similar to that of the wild type.

Next, we examined the effect of the used pretreatments on the matrix polysaccharide (consisting mainly of hemi-cellulose) and lignin content in *ccr2 ProSNBE:AtCCR1* line 18 and wild-type poplars; although both pretreatments extracted matrix polysaccharides and lignin from the cell wall of both genotypes, the acid pretreatment extracted predominantly matrix polysaccharides while the alkaline pretreatment extracted mainly lignin (Figure S6a, b). We also focused on the relative differences in matrix polysaccharide and lignin extraction efficiency of both pretreatments between the two genotypes; the acid pretreatment extracted relatively more matrix polysaccharides from the cell wall of *ccr2 ProSNBE:AtCCR1* line 18 than from the cell wall of wild-type poplar, while extracting similar relative amounts of lignin from both genotypes (Figure S6c, d). The alkaline pretreatment extracted similar relative amounts of matrix polysaccharides and lignin from the cell wall of both genotypes (Figure S6c, d).

Finally, the cellulose accessibility and biomass porosity were examined for *ccr2 ProSNBE:AtCCR1* line 18 and wild type as these parameters have been shown to be important determinants of biomass enzymatic hydrolysis potential (Zhang et al., 2020). The cellulosic surface area, estimated by using the Congo-red staining approach, was significantly increased in *ccr2 ProSNBE:AtCCR1* line 18 compared to the wild type

indicating that this line has more surface sites for cellulase enzyme attack (Figure S7a). Determination of the biomass porosity using Simons' staining showed an increased yellow dye staining and an equal blue dye staining in *ccr2 ProSNBE:AtCCR1* line 18 compared to the wild type, revealing an increased number of large-size pores in *ccr2 ProSNBE:AtCCR1* line 18 stem biomass (Figure S7b, c). Given the negative correlation between lignin amount on the one hand, and biomass porosity and saccharification efficiency on the other hand, the increased saccharification potential of *ccr2 ProSNBE:AtCCR1* line 18 could be largely attributed to these factors, but possibly also to the increased levels of ferulic acid and H units in its lignin polymer (Ziebell et al., 2010; Van Acker et al., 2013; Lv et al., 2021; Zhang et al., 2021).

DISCUSSION

ProSNBE directs expression not solely to the vessels, but also to the rays in poplar

AtXCP1 and *BdXCP1* promoter sequences direct expression specifically in vessel elements in *Arabidopsis thaliana* and *Brachypodium distachyon*, respectively (Funk et al., 2002; Zhong et al., 2010; Valdivia et al., 2013). This specific expression pattern is imposed by the presence of *SNBE*s, which are conserved imperfect palindromic 19-bp-long promoter elements that interact with transcription factors involved in secondary cell wall biosynthesis (Zhong et al., 2010). *XCP1* promoter deletion analyses in Arabidopsis and Brachypodium showed that at least two *SNBE*s are required to specify the vessel-specific expression pattern (Zhong et al., 2010; Valdivia et al., 2013). Moreover, analysis of an artificial promoter consisting of three tandem repeats of the Arabidopsis *XCP1-SNBE* (*ProSNBE*) showed that solely (multiple) *SNBE*s and a minimal promoter (but no other *XCP1* promoter elements) are essential to achieve the vessel-specific expression pattern (McCarthy et al., 2011; De Meester et al., 2018).

As *XCP1-SNBE*s confer expression in the vessels of Arabidopsis and Brachypodium, we investigated whether *ProSNBE* would also direct expression to the vessel (and not the fiber) cells of poplar. In contrast to in Arabidopsis and Brachypodium, GUS activity in *ProSNBE:GUS* poplars was not only restricted to developing vessels, but was also detected in (predominantly contact) ray cells. Nevertheless, it appeared that *SNBE*s present in the *AtXCP1* promoter did not confer expression in fiber cells of poplar, making it an interesting promoter to study monolignol

transport to fibers and to possibly achieve increased vessel lignification and fiber hypolignification.

Poplar vessel and ray cells act as good neighbors in lignification

In *ccr1 ProSNBE:AtCCR1* Arabidopsis plants, *CCR1* expression (and thus monolignol biosynthesis) was restricted to the vessels (De Meester et al., 2018). Nevertheless, lignin deposition was partially restored in both vessels and xylary fibers, but not in the interfascicular fibers. The latter implies that (i) Arabidopsis xylem cells can interchange monolignols, and (ii) Arabidopsis interfascicular fibers are not capable of receiving monolignols from the xylem in *ccr1 ProSNBE:AtCCR1* Arabidopsis lines. This suggests either that a yet unknown barrier limits the translocation of monomers from the xylem region to the interfascicular fiber region in Arabidopsis, or -more likely- that the monolignols might all be trapped in the cell wall of the vessel cells producing them, and their adjoining xylary fiber cells. The latter is supported by the observation that lignin levels in vessels and xylary fibers of *ccr1 ProSNBE:AtCCR1* Arabidopsis lines were still lower than those of corresponding wild-type cells, hinting that there was still room for trapping monolignols into xylary cell walls, and thus preventing them from being transported towards walls of interfascicular fiber cells.

The analysis of *ccr2 ProSNBE:AtCCR1* poplars revealed that good neighbors for lignification also exist in poplar. More specifically, studying *ccr2 ProSNBE:AtCCR1* lines 3 and 10 showed that monolignols are able to migrate over multiple cell layers as, next to the fibers adjoining the monolignol-producing vessels and rays, also non-adjoining fibers showed an increased lignin deposition. Even more, it is possible to restore lignin amounts in non-monolignol-producing fibers to wild-type levels as long as the vessels and rays biosynthesize sufficient monolignols.

Studying *ccr2 ProSNBE:AtCCR1* line 18 has shown that if the supply of monolignols is limited, the monolignols are not distributed equally over all xylem cell (wall)s, but are trapped by the cell wall of the cells producing them and their adjoining cells. This is in line with the observation in *ccr1 ProSNBE:AtCCR1* Arabidopsis lines, where the monolignols are not distributed equally over all secondary cell walls, but are trapped by the hypolignified cell walls of xylary cells.

Previous analyses of transgenic poplar lines overexpressing an engineered form of the lignin-biosynthesis repressor *LIGNIN BIOSYNTHESIS ASSOCIATED TRANSCRIPTION FACTOR 1* (*LTF1*) has provided us more insight into the

radicalization status of the monolignols upon migration to neighboring cells (Gui et al., 2020). In *Populus deltoides* × *P. euramericana,* a phosphorylation-null mutant version of *LTF1* (*LTF1*^{AA}) was expressed in the fibers. This most likely resulted in a suppression of all genes involved in lignin biosynthesis in fibers, including genes coding for the cell-wall localized laccases and peroxidases involved in dehydrogenation of the lignin monomers, in contrast to the *ccr2 ProSNBE:AtCCR1* lines in which the monolignol dehydrogenation machinery is still present in fibers. The observation that lignin deposition in *LTF1*^{AA} poplars was restricted to the vessel cells, and was not also observed in adjoining and non-adjoining fibers as in our study, suggests that the non-radicalized monomers rather than the radicalized monomers migrate through the cells and cell walls to neighboring cell walls. In poplar lines with a fiber-specific overexpression of the *LTF1*^{AA} repressor, the lignin monomers can only be dehydrogenated in vessel walls, where the laccases and peroxidases are still present. Seemingly, the oxidized monomers couple shortly after their oxidation, rather than migrate to neighboring cell walls.

Is vessel (and ray)- specific lignin biosynthesis a promising approach to engineer fiber-hypolignification in poplar?

ccr2 ProSNBE:AtCCR1 lines 3 and 10 had a vessel integrity, growth, lignin amount and saccharification efficiency equal to that of the wild type. *ccr2 ProSNBE:AtCCR1* line 18 also demonstrated a largely restored vessel integrity and growth, but was hypolignified in the fiber cells. The latter was the consequence of its lower *AtCCR1* expression level (as compared to that of the other *ccr2 ProSNBE:AtCCR1* lines). Such variation in transgene expression is expected for different insertion events. The lignin amount in *ccr2 ProSNBE:AtCCR1* line 18 was stably reduced, as all biological replicates displayed a uniform red coloration of the xylem along the stem. Overall, *ccr2 ProSNBE:AtCCR1* line 18 had an 18% reduction in lignin amount (which was not compensated by an increased cellulose or matrix polysaccharide amount) and despite its yield penalty, still had an increase of up to 71% in sugar release on a per plant base after saccharification. Recently, another stable CCR2-deficient poplar line was made by CRISPR/Cas9 (De Meester et al., 2020). This line that combined a null mutation in one of the two *CCR2* alleles with a haploinsufficient mutation in the other allele, had a 10% reduction in lignin amount and an increase of up to 41% in sugar release on a per plant base upon saccharification,

while growth was normal. These observations illustrate that a relatively small yield penalty, as compared to the e.g. severe yield penalty of *ccr2* knock-out poplars, does not necessarily fully offset the gain in saccharification yield. Even more, lines with a relatively small yield penalty might need less severe, and thus less costly pretreatments to yield the same amount of sugar upon saccharification.

The results shown here suggest that the followed strategy, i.e. tissue-specific expression of a monolignol biosynthesis gene in the corresponding mutant background leading to hypolignification in the fibers, is interesting for designing low-lignin trees for the biorefinery. However, we have to note that although *AtCCR1* expression - and, hence, monolignol production - in all *ccr2 ProSNBE:AtCCR1* lines was restricted to vessels and rays, most of them showed a complete recovery in lignin deposition due to the existence of good neighbors for lignification in poplar. Although the latter complicates tissue-specific lignification in poplar, it was shown that it is still possible to achieve hypolignification in fibers in *ccr2 ProSNBE:AtCCR1* lines as long as *AtCCR1* expression and thus the amount of monolignols produced by vessels and rays is limited (e.g. as in *ccr2 ProSNBE:AtCCR1* line 18). Here, the fiber-hypolignified *ccr2 ProSNBE:AtCCR1* line 18 displayed a relatively small yield penalty. However, in practice, the variation in transgene expression expected among individual transgenic events might be sufficient to select a line with reduced lignin content and higher saccharification efficiency, but without yield penalty. To enrich for lines that do not fully restore lignin amount in the fibers, one strategy could be to make use of an alternative tissue-specific promoter that has a lower activity than that of *ProSNBE*. For example, as it has been shown that two copies of *XCP1-SNBE*s are sufficient for promoter activity (Zhong et al., 2010; Valdivia et al., 2013), reducing the number of *SNBE*s in *ProSNBE* from three to two might reduce promoter activity. An alternative strategy might involve reducing the activity of the monolignol biosynthesis enzyme used for the complementation approach by e.g. engineering a weak allele of the corresponding gene, as described by De Meester et al. (2020).

EXPERIMENTAL PROCEDURES

Vector construction and poplar (*P. tremula* x *P. alba*) transformation

The *ProSNBE:GUS* construct was previously described in De Meester et al. (2018). In short, the *ProSNBE* building block was introduced into the destination vector

*pMK7S*NFm14GW*, which fused *ProSNBE* to a *NUCLEAR LOCALIZATION SIGNAL*:*GREEN FLUORESCENT PROTEIN*:*GUS* reporter construct.

The generation and analysis of *ccr2* poplars was previously described in De Meester et al. (2020). In short, the *p201N-Cas9:gRNA1_CCR2* construct was generated by cloning guide RNA 1 (gRNA1) GACCAAAAATGTGATCATTG into the *p201N-Cas9* vector. gRNA1 targets the third exon of both *CCR2* (Potri.003G181400) alleles.

For the generation of the *ccr2 ProSNBE:AtCCR1* poplars, subsequent cloning steps were required to introduce the *ProSNBE:AtCCR1* construct into the *p201N-Cas9:gRNA1_CCR2* vector. To achieve this, the *ProSNBE:AtCCR1* expression clone (described in De Meester et al., 2018) was used to amplify *ProSNBE:AtCCR1* using primers containing the *Spe*I restriction site. Subsequently, the PCR product was cloned into the digested *p201N-Cas9:gRNA1_CCR2* using T4 DNA Ligase (Invitrogen), yielding the *p201N-Cas9:gRNA1_CCR2:ProSNBE:AtCCR1* construct.

The *ProSNBE:GUS*, *p201NCas9:gRNA_CCR2* and *p201N-Cas9:gRNA_CCR2:ProSNBE:AtCCR1* expression clones were all transferred into *Agrobacterium tumefaciens* strain C58C1 660 PMP90 by electroporation and positive colonies were selected via PCR. Agrobacterium-mediated transformation of *P. tremula* × *P. alba* 717-1B4 was performed according to Leplé et al. (1992). The identification of transformed plants was based on kanamycin resistance. The insertion of the transgenes was confirmed by PCR, followed by gel electrophoresis.

Plant growth and harvest

All *ProSNBE:GUS* lines originated from different calli and were therefore biologically independent. Most of the *ccr2 ProSNBE:AtCCR1* plantlets originated from different calli (indicated in Figure S3 with different (starting) numbers, e.g. line 1 and line 2). However, some plantlets originated from the same calli (indicated in Figure S3 with the same starting numbers, e.g. line 22-1 and line 22-2). Plantlets originating from the same callus might be biologically dependent. However, the different indel pattern in *CCR2* for the *ccr2 ProSNBE:AtCCR1* plantlets originating from the same callus showed that all *ccr2 ProSNBE:AtCCR1* lines were biologically independent.

The *ProSNBE:GUS* lines, *ccr2 ProSNBE:AtCCR1* plantlets and wild-type control poplars were first grown for four months on half-strength Murashige and Skoog (1/2 MS) medium in long-day conditions (16-h light/ 8-h dark photoperiod, 21°C, 55%

humidity). After genotyping, the *in vitro*-grown plants were individually transferred to soil in pots of 5.5-cm diameter, placed in a tray filled with water and covered with a cage liner (Tecniplast APET disposable cage liner for cage body 1291H) for acclimatization. After two weeks, one side of the cage liner was lifted above the water level to allow aeration and kept accordingly for four days, after which the other side was also lifted above the water level for a period of three days. The next day, the cage liner was removed and the acclimatized plants were transferred to bigger pots (24-cm diameter) and grown in randomized locations within the greenhouse until they reached a height of approximately 2 m (after five months). For the initial selection of *ccr2 ProSNBE:AtCCR1* lines, the 15 biologically independent lines and their wild-type controls were harvested by cutting the stem 15 cm above the soil, leaving two to three axillary buds to allow development of new shoots. For microscopy, the part ranging from 15 cm to 20 cm relative to the soil was debarked and kept in tap water. The samples were analyzed within 4 h. Next, the top 20 cm of the stem was removed. For cell wall analysis and saccharification, the leftover stem piece (being the stem piece ranging from 20 cm relative to the soil to 20 cm relative to the top of the stem) was debarked, air-dried and ground in a ball mill.

Three *ccr2 ProSNBE:AtCCR1* lines were selected and, together with wild-type controls, simultaneously vegetatively propagated and grown in the greenhouse to obtain multiple biological replicates for each line. After five months of growth, they reached a height of approximately 2 m. All poplars were harvested by cutting the stem 15 cm above the soil leaving two to three axillary buds to allow development of new shoots. For microscopy, the 5-cm stem piece between 25 and 30 cm relative to the soil level was stored in 70% ethanol. The samples were analyzed after two weeks. For RT-qPCR, the 5-cm stem piece between 30 and 35 cm was debarked, snap-frozen in liquid nitrogen and stored at -70 °C. For cell wall analysis and saccharification, the stem piece between 35 cm relative to the soil and 20 cm relative to the top of the stem was debarked, left to air-dry for three weeks, and ground in a ball mill.

Reporter gene analysis

After growing the *ProSNBE:GUS* lines for five months in the greenhouse, the part of the stem ranging from 20 to 15 cm relative to the top was harvested for GUS analysis. The 5-cm pieces were embedded in 7% agarose, and sliced into stem sections of approximately 100 nm in thickness with a vibratome (Campden

Instruments, Loughborough, United Kingdom). After being cut, the sections were directly submerged in cold 70% ethanol to suppress the wound response. To screen for GUS staining, the sections were incubated in the dark at 37°C for 15 to 60 min in freshly prepared X-Gluc solution [1.0 mM X-Gluc, 0.5% dimethylformamide, 0.5% Trition X-100, 1.0 mM EDTA (pH 8), 0.5 mM $K_3Fe(CN)_6$ and 0.5 mM $K_4Fe(CN)_6$ in 500 mM Na_2PO_4 buffer (pH 7)], and analyzed with a binocular microscope (model Bino Leica MZ16, Leica, Diegem, Belgium).

Microscopy

Slices of 15-µm-thick *ccr2 ProSNBE:AtCCR1* stems were made using a Reichert-Jung 2040 Autocut Microtome (Leica, Diegem, Belgium). The sections were imaged with Mäule or Wiesner staining as described in Pradhan, Mitra and Loqué (2014). Images were acquired using a Zeiss Axioskop 2 microscope with an EC Plan-Neofluar 20X (0.5 dry) objective.

Gene expression analysis via RT-qPCR

Frozen stems were scraped with a scalpel. Subsequently, the xylem material (which was removed from the stem piece with a scalpel) was ground to fine powder using a mortar/pestle and a Retsch MM300 mill (20 Hz, 5-mm bead). Total RNA was isolated using the ReliaPrep™ RNA Tissue Miniprep System (Promega). To eliminate genomic DNA contamination, on-column DNase digestion was performed (included in the ReliaPrep™ RNA Tissue Miniprep System (Promega)). RNAs from two plants were pooled to constitute a replicate. Total RNA (1 µg) was used as a template for the synthesis of cDNA using qScript® cDNA SuperMix (Quantabio). The transcript levels of *AtCCR1* (AT1G15950) were determined with the Roche LightCycler 480 combined with the SYBR Green I Master Kit (Roche Diagnostics) in three technical repeats. Poplar *18S RIBOSOMAL RNA* (AF206999), *POLYUBIQUITIN* (BU879229), and *LEAFY/FLORICAULA* (Potri.015G106900) were used as reference genes. All primers used in this study are listed in Table S2. For the statistical analysis, normalized relative quantities were log10 transformed.

Cell wall characterization and saccharification

To determine the cellulose, matrix polysaccharide, and lignin characteristics, ground powder was used for preparing cell wall residue by sequentially washing for 30 min each with milliQ water at 98 °C, ethanol at 76 °C, chloroform at 59 °C, and acetone

at 54 °C. The remaining CWR was dried under vacuum. To determine the crystalline cellulose amount, the Updegraff method was used on 10 mg of CWR essentially as described by Updegraff (1969) and modified according to De Meester et al. (2020). The weight loss upon trifluoroacetic acid digestion was used to determine the matrix polysaccharide content (including mainly hemicelluloses, but also pectins and amorphous cellulose). Lignin content was determined by the acetyl bromide method on 5 mg of CWR essentially as described by Dence (1992) and modified according to Van Acker et al. (2013). Lignin composition was determined via thioacidolysis on 15 mg of CWR as previously described by Robinson et al. (2009).

Saccharification was performed on 10 mg of dried, ground stem material as described by Van Acker et al. (2016). The samples were saccharified for 48 h using no pretreatment, acid pretreatment (1 M HCl, 80 °C for 2 h while shaking at 750 rpm), or alkaline pretreatment (62.5 mM NaOH, 90 °C for 3 h while shaking at 750 rpm). The glucose yield per plant was calculated using the dry weight of the debarked stem.

Cellulose accessibility and biomass porosity measurements

Congo red stain to evaluate the cellulose accessibility was performed as described by Zhang et al. (2020). In short, 100 mg of biomass sample (dried, ground stem material) was incubated with dye solution at a series of concentrations (0.5, 1.0, 2.0, 3.0, 4.0, 5.0 g/L) in phosphate-buffered saline solution (PBS; pH 6) at 60°C for 24 h while shaking at 200 rpm. After centrifugation at 8,000 g, the absorbance of the supernatant was measured at 498 nm. The cellulosic surface area was estimated from the maximum adsorption capacities by assuming that direct red adsorbs as dimer aggregates under experimental conditions. The maximum dye adsorption capacity of the biomass was calculated using the monolayer Langmuir adsorption model as previously described by Chandra et al. (2008).

Simons' stain was applied to determine the overall biomass porosity as described in Zhang et al. (2020). Direct Blue 15 (DB) and Direct Yellow 11 (DY) were purchased from Sigma. In short, 100 mg of biomass sample (dried, ground stem material) was incubated with 1 ml of PBS (pH 6), a 1:1 solution of DB and DY (prepared by adding the dye solution (10 mg/ml) in a series of volumes (0.25, 0.50, 0.75, 1.0, 1.5 ml)) and milliQ water to a total volume of 10 ml. After incubating the samples for 9 h at 70°C while shaking at 200 rpm, they were centrifuged at 8,000 g. The absorbances of the supernatants were measured at 612 nm and 410 nm (the wavelengths of

maximum absorbance for DB and DY). The concentration of DB and DY dyes in the supernatants was calculated according to the Lambert–Beer law for binary solutions. The maximum DB and DY dyes adsorbed to the biomasses were calculated using the Langmuir adsorption model as previously described by Chandra et al. (2008).

AUTHOR CONTRIBUTIONS

B.D.M., R.V. and W.B. designed the research. B.D.M. and L.d.V. performed the experiments by cloning the constructs, J.V.D. performed the experiments by generating the transgenic poplars, B.D.M. performed the experiments by analyzing the transgenic plants through reporter gene -, growth -, microscopic -, cell wall - and saccharification analysis, M.W. performed the RT-qPCR experiments. B.D.M. performed the data analysis. B.D.M., R.V. and W.B. wrote the article. W.B. agrees to serve as the author responsible for contact and ensures communication.

ACKNOWLEDGEMENTS

We thank Annick Bleys for helping in preparing the manuscript. B.D.M. was funded by the Institute for the Promotion of Innovation through Science and Technology in Flanders (IWT-Vlaanderen) for a predoctoral fellowship and the Research Foundation Flanders (FWO) for a postdoctoral fellowship, M.W. was funded by FWO for a predoctoral fellowship, L.d.V. was funded by IWT-Vlaanderen for a predoctoral fellowship, R.V. was funded by FWO for a postdoctoral fellowship.

CONFLICT OF INTEREST

The authors declare no conflict of interest

SUPPORTING INFORMATION

Additional Supporting Information may be found online in the Supporting Information tab of this article:

Figure S1. Expression pattern conferred by *ProSNBE* in poplar stems.

Figure S2. Phenotype of wild-type and *ccr2* poplars grown for 5 months in the greenhouse.

Figure S3. Sequence information of the targeted *CCR2* locus of *ccr2 ProSNBE:AtCCR1* poplars (*P. tremula x P. alba*).

Figure S4. Protein sequence corresponding to the mutated *P. tremula* and *P. alba CCR2* alleles of the selected *ccr2 ProSNBE:AtCCR1* lines.

Figure S5. Lignin deposition in the non-selected *ccr2 ProSNBE:AtCCR1* poplars.

Figure S6. Effect of saccharification pretreatments on matrix polysaccharide and lignin levels in wild type and *ccr2 ProSNBE:AtCCR1* line 18.

Figure S7. Characterization of cellulose accessibility and biomass porosity in wild type and *ccr2 ProSNBE:AtCCR1* line 18.

Table S1. Screening for the best-performing *ccr2 ProSNBE:AtCCR1* lines based on sugar yield after saccharification.

Table S2. Primers used for RT-qPCR of the *ccr2 ProSNBE:AtCCR1* lines.

Note S1. Microscopic analysis of additional *ccr2 ProSNBE:AtCCR1* lines.

REFERENCES

Bonawitz ND, Chapple C (2013) Can genetic engineering of lignin deposition be accomplished without an unacceptable yield penalty? Curr Opin Biotechnol **24:** 336-343

Bonawitz ND, Kim JI, Tobimatsu Y, Ciesielski PN, Anderson NA, Ximenes E, Maeda J, Ralph J, Donohoe BS, Ladisch M, Chapple C (2014) Disruption of mediator rescues the stunted growth of a lignin-deficient Arabidopsis mutant. Nature **509**: 376-380

Chandel AK, Garlapati VK, Singh AK, Antunes FAF, da Silva SS (2018) The path forward for lignocellulose biorefineries: bottlenecks, solutions, and perspective on commercialization. Bioresour Technol **264:** 370-381

Chandra R, Ewanick S, Hsieh C, Saddler JN (2008) The characterization of pretreated lignocellulosic substrates prior to enzymatic hydrolysis, part 1: a modified Simons' staining technique. Biotechnol **24(5):** 1178-85

Chanoca A, de Vries L, Boerjan W (2019) Lignin engineering in forest trees. Front Plant Sci **10:** 912

Chen C, Meyermans H, Burggraeve B, De Rycke RM, Inoue K, De Vleesschauwer V, Steenackers M, Van Montagu MC, Engler GJ, Boerjan WA (2000) Cell-specific and conditional expression of caffeoyl-coenzyme A-3-*O*-methyltransferase in poplar. Plant Physiology **123:** 853-867

Chen F, Dixon RA (2007) Lignin modification improves fermentable sugar yields for biofuel production. Nat Biotechnol **25:** 759-761

De Meester B, de Vries L, Özparpucu M, Gierlinger N, Corneillie S, Pallidis A, Goeminne G, Morreel K, De Bruyne M, De Rycke R, et al (2018) Vessel-specific reintroduction of CINNAMOYL-COA REDUCTASE1 (CCR1) in dwarfed *ccr1* mutants restores vessel and xylary fiber integrity and increases biomass. Plant Physiol **176:** 611-633

De Meester B, Madariaga Calderón B, de Vries L, Pollier J, Goeminne G, Van Doorsselaere J, Chen M, Ralph J, Vanholme R, Boerjan W (2020) Tailoring poplar lignin without yield penalty by combining a null and haploinsufficient CINNAMOYL-CoA REDUCTASE2 allele. Nat Commun **11(1):** 5020

Dence C. (1992) Lignin determination. Methods in Lignin Chemistry: 33–61 (Springer-Verlag, Berlin, Germany)

Funk V, Kositsup B, Zhao C, Beers EP (2002) The Arabidopsis xylem peptidase XCP1 is a tracheary element vacuolar protein that may be a papain ortholog. Plant Physiol **128:** 84-94

Gallego-Giraldo L, Escamilla-Trevino L, Jackson LA, Dixon RA (2011) Salicylic acid mediates the reduced growth of lignin down-regulated plants. Proc Natl Acad Sci U S A **108:** 20814-20819

Gorzsás A, Stenlund H, Persson P, Trygg J, Sundberg B (2011) Cell-specific chemotyping and multivariate imaging by combined FT-IR microspectroscopy and orthogonal projections to latent structures (OPLS) analysis reveals the chemical landscape of secondary xylem. Plant J **66:** 903-914

Goujon T, Ferret V, Mila I, Pollet B, Ruel K, Burlat V, Joseleau J-P, Barrière Y, Lapierre C, Jouanin L (2003) Down-regulation of the *AtCCR1* gene in *Arabidopsis thaliana*: effects on phenotype, lignins and cell wall degradability. Planta **217:** 218-228

Gui J, Lam PY, Tobimatsu Y, Sun J, Huang C, Cao S, Zhong Y, Umezawa T, Li L (2020) Fibre-specific regulation of lignin biosynthesis improves biomass quality in Populus. New Phytologist **226(4):**1074-1087

Ha CM, Rao X, Saxena G, Dixon RA (2021) Growth-defense trade-offs and yield loss in plants with engineered cell walls. New Phytologist **231(1):** 60-74

Hosokawa M, Suzuki S, Umezawa T, Sato Y (2001) Progress of lignification mediated by intercellular transportation of monolignols during tracheary element differentiation of isolated *Zinnia* mesophyll cells. Plant Cell Physiol **42:** 959-968

Klein-Marcuschamer D, Oleskowicz-Popiel P, Simmons BA, Blanch HW (2012) The challenge of enzyme cost in the production of lignocellulosic biofuels Biotechnol Bioeng **109(4):** 1083-1087

Larisch C, Dittrich M, Wildhagen H, Lautner S, Fromm J, Polle A, Hedrich R, Rennenberg H, Müller T, Ache P (2012) Poplar wood rays are involved in seasonal remodeling of tree physiology. Plant Physiol **160:** 1515-1529

Leplé J-C, Dauwe R, Morreel K, Storme V, Lapierre C, Pollet B, Naumann A, Kang K-Y, Kim H, Ruel K, et al (2007) Downregulation of cinnamoyl-coenzyme A reductase in poplar: multiple-level phenotyping reveals effects on cell wall polymer metabolism and structure. Plant Cell **19:** 3669-3691

Leplé JC, Brasileiro ACM, Michel MF, Delmotte F, Jouanin L (1992) Transgenic poplars: expression of chimeric genes using four different constructs. Plant Cell Rep **11:** 137-141

Linger JG, Vardon DR, Guarnieri MT, Karp EM, Hunsinger GB, Franden MA, Johnson CW, Chupka G, Strathmann TJ, Pienkos PT (2014) Lignin valorization through integrated biological funneling and chemical catalysis. Proc Natl Acad Sci USA **111:** 12013-12018

Liu X, Van Acker R, Voorend W, Pallidis A, Goeminne G, Pollier J, Morreel K, Kim H, Muylle H, Bosio M, Ralph J, Vanholme R, Boerjan W (2021) Rewired phenolic metabolism and improved saccharification efficiency of a *Zea mays cinnamyl alcohol dehydrogenase 2* (*zmcad2*) mutant. Plant J **105(5):** 1240-1257

Lv ZY, Liu F, Zhang YB, Tu YY, Chen P, Peng LC (2021) Ecologically adaptable Populus simonii is specific for recalcitrance-reduced lignocellulose and largely enhanced enzymatic saccharification among woody plants. Gcb Bioenergy **13:** 348-360

Mahon EL, Mansfield SD (2019) Tailor-made trees: engineering lignin for ease of processing and tomorrow's bioeconomy. Curr Opin Biotechnol **56:** 147-155

Marriott PE, Gómez LD, McQueen-Mason SJ (2016) Unlocking the potential of lignocellulosic biomass through plant science. New Phytol **209:** 1366-1381

Maurya DP, Singla A, Negi S (2015) An overview of key pretreatment processes for biological conversion of lignocellulosic biomass to bioethanol. 3 Biotech **5:** 597-609

McCarthy RL, Zhong R, Ye Z-H (2011) Secondary wall NAC binding element (SNBE), a key cis-acting element required for target gene activation by secondary wall NAC master switches. Plant Signal Behav **6:** 1282-1285

Mir Derikvand M, Berrio Sierra J, Ruel K, Pollet B, Do C-T, Thévenin J, Buffard D, Jouanin L, Lapierre C (2008) Redirection of the phenylpropanoid pathway to feruloyl malate in *Arabidopsis* mutants deficient for cinnamoyl-CoA reductase 1. Planta **227:** 943-956

Mottiar Y, Vanholme R, Boerjan W, Ralph J, Mansfield SD (2016) Designer lignins: harnessing the plasticity of lignification. Curr Opin Biotechnol **37:** 190-200

Murakami Y, Funada R, Sano Y, Ohtani J (1999) The differentiation of contact cells and isolation cells in the xylem ray parenchyma of *Populus maximowiczii*. Ann Bot **84:** 429-435

Muro-Villanueva F, Mao X, Chapple C (2019) Linking phenylpropanoid metabolism, lignin deposition, and plant growth inhibition. Curr Opin Biotechnol **56:** 202-208

Oyarce P, De Meester B, Fonseca F, de Vries L, Goeminne G, Pallidis A, De Rycke R, Tsuji Y, Li Y, Van den Bosch S, et al (2019) Introducing curcumin biosynthesis in *Arabidopsis* enhances lignocellulosic biomass processing. Nat Plants **5:** 225-237

Perkins M, Smith RA, Samuels L (2019) The transport of monomers during lignification in plants: anything goes but how? Curr Opin Biotechnol **56:** 69-74

Pesquet E, Zhang B, Gorzsás A, Puhakainen T, Serk H, Escamez S, Barbier O, Gerber L, Courtois-Moreau C, Alatalo E, et al (2013) Non-cell-autonomous postmortem lignification of tracheary elements in *Zinnia elegans*. Plant Cell **25:** 1314-1328

Pradhan Mitra P, Loqué D (2014) Histochemical staining of *Arabidopsis thaliana* secondary cell wall elements. J Vis Exp **(87):** e51381, doi: 51310.53791/51381

Ralph J, Kim H, Lu F, Grabber JH, Leplé J-C, Berrio-Sierra J, Mir Derikvand M, Jouanin L, Boerjan W, Lapierre C (2008) Identification of the structure and origin of a thioacidolysis marker compound for ferulic acid incorporation into angiosperm lignins (and an indicator for cinnamoyl CoA reductase deficiency). Plant J **53:** 368-379

Rinaldi R, Jastrzebski R, Clough MT, Ralph J, Kennema M, Bruijnincx PCA, Weckhuysen BM (2016) Paving the way for lignin valorisation: Recent advances in bioengineering, biorefining and catalysis. Angew Chem Int Ed **55:** 8164-8215

Robinson AR, Mansfield SD (2009) Rapid analysis of poplar lignin monomer composition by a streamlined thioacidolysis procedure and near-infrared reflectance-based prediction modeling. Plant J **58**: 706–714

Schilmiller AL, Stout J, Weng JK, Humphreys J, Ruegger MO, Chapple C (2009) Mutations in the *cinnamate 4-hydroxylase* gene impact metabolism, growth and development in Arabidopsis. Plant J **60:** 771-782

Schutyser W, Renders T, Van den Bosch S, Koelewijn S-F, Beckham GT, Sels BF (2018) Chemicals from lignin: an interplay of lignocellulose fractionation, depolymerisation, and upgrading. Chem Soc Rev **47:** 852-908

Silva COG, Vaz RP, Filho EXF (2018) Bringing plant cell wall-degrading enzymes into the lignocellulosic biorefinery concept. Biofuels, Bioprod Bioref **12:** 277-289

Smith RA, Schuetz M, Karlen SD, Bird D, Tokunaga N, Sato Y, Mansfield SD, Ralph J, Samuels AL (2017) Defining the diverse cell populations contributing to lignification in Arabidopsis stems. Plant Physiol **174:** 1028-1036

Smith RA, Schuetz M, Roach M, Mansfield SD, Ellis B, Samuels L (2013) Neighboring parenchyma cells contribute to *Arabidopsis* xylem lignification, while lignification of interfascicular fibers is cell autonomous. Plant Cell **25:** 3988-3999

Tobimatsu Y, Schuetz M (2019) Lignin polymerization: how do plants manage the chemistry so well? Curr Opin Biotech **56:** 75-81

Tokunaga N, Sakakibara N, Umezawa T, Ito Y, Fukuda H, Sato Y (2005) Involvement of extracellular dilignols in lignification during tracheary element differentiation of isolated *Zinnia* mesophyll cells. Plant Cell Physiol **46:** 224-232

Updegraff DM (1969) Semimicro determination of cellulose in biological materials. Anal Biochem **32:** 420–424

Valdivia ER, Herrera MT, Gianzo C, Fidalgo J, Revilla G, Zarra I, Sampedro J (2013) Regulation of secondary wall synthesis and cell death by NAC transcription factors in the monocot *Brachypodium distachyon*. J Exp Bot **64:** 1333-1343

Van Acker R, Leplé J-C, Aerts D, Storme V, Goeminne G, Ivens B, Légée F, Lapierre C, Piens K, Van Montagu MCE, et al (2014) Improved saccharification and ethanol yield from field-grown transgenic poplar deficient in cinnamoyl-CoA reductase. Proc Natl Acad Sci USA **111:** 845-850

Van Acker R, Vanholme R, Piens K, Boerjan W (2016) Saccharification protocol for small-scale lignocellulosic biomass samples to test processing of cellulose into glucose. Bio-Protoc **6:** e1701

Van Acker R, Vanholme R, Storme V, Mortimer JC, Dupree P, Boerjan W (2013) Lignin biosynthesis perturbations affect secondary cell wall composition and saccharification yield in *Arabidopsis thaliana*. Biotechnol Biofuels **6:** 46

Vanholme B, Desmet T, Ronsse F, Rabaey K, Van Breusegem F, De Mey M, Soetaert W, Boerjan W (2013a) Towards a carbon-negative sustainable bio-based economy. Front Plant Sci **4:** 174

Vanholme R, Cesarino I, Rataj K, Xiao Y, Sundin L, Goeminne G, Kim H, Cross J, Morreel K, Araujo P, et al (2013b) Caffeoyl shikimate esterase (CSE) is an

enzyme in the lignin biosynthetic pathway in *Arabidopsis*. Science **341:** 1103-1106

Vanholme R, De Meester B, Ralph J, Boerjan W (2019) Lignin biosynthesis and its integration into metabolism. Curr Opin Biotechnol **56:** 230-239

Vargas L, Cesarino I, Vanholme R, Voorend W, de Lyra Soriano Saleme M, Morreel K, Boerjan W (2016) Improving total saccharification yield of Arabidopsis plants by vessel-specific complementation of *caffeoyl shikimate esterase* (*cse*) mutants. Biotechnol Biofuels **9:** 139

Vermaas JV, Dixon RA, Chen F, Mansfield SD, Boerjan W, Ralph J, Crowley MF, Beckham GT (2019) Passive membrane transport of lignin-related compounds. Proc Natl Acad Sci USA **116:** 23117-23123

Wang Y, Chantreau M, Sibout R, Hawkins S (2013) Plant cell wall lignification and monolignol metabolism. Front Plant Sci **4:** 220

Yang F, Mitra P, Ling Z, Prak L, Verhertbruggen Y, Kim J-S, Sun L, Zheng K, Tang K, Auer M, et al (2013) Engineering secondary cell wall deposition in plants. Plant Biotechnol J **11:** 325-335

Zhang GF, Wang LQ, Li XK, Bai SM, Xue YL, Li ZH, Tang SW, Wang YT, Wang YM, Hu Z, et al (2021) Distinctively altered lignin biosynthesis by site-modification of OsCAD2 for enhanced biomass saccharification in rice. Gcb Bioenergy **13:** 305-319

Zhong R, Lee C, Ye Z-H (2010) Global analysis of direct targets of secondary wall NAC master switches in *Arabidopsis*. Mol Plant **3:** 1087-1103

Ziebell A, Gracom K, Katahira R, Chen F, Pu Y, Ragauskas A, Dixon RA, Davis M (2010) Increase in 4-coumaryl alcohol units during lignification in alfalfa (Medicago sativa) alters the extractability and molecular weight of lignin. J Biol Chem **285**: 38961–38968

TABLES

Table 1. Biomass measurements of *ccr2 ProSNBE:AtCCR1* poplars. Measurements were performed on poplars grown for five months in the greenhouse. Stem diameter was determined 10 cm above soil level. Fresh weight of the stem (without leaves) was determined with and without bark. Dry weight of the stem was determined without leaves and bark. Different letters represent significant differences at the 0.05 significance level (One-way ANOVA with Tukey's post-hoc test; n = 6 biologically independent samples for wild type, *ccr2 ProSNBE:AtCCR1* lines 3 and 10; n = 8 biologically independent samples for *ccr2 ProSNBE:AtCCR1* line 18). All values are given as means ± standard deviation.

	Wild type	***ccr2 ProSNBE:AtCCR1* line 3**	***ccr2 ProSNBE:AtCCR1* line 10**	***ccr2 ProSNBE:AtCCR1* line 18**
Height (cm)	198.7 ± 5.2 a	197.8 ± 5.2 a	205.1 ± 5.2 a	175.5 ± 4.5 b
Fresh weight with bark (g)	62.2 ± 18.0 a	73.9 ± 18.7 a	74.7 ± 12.9 a	56.8 ± 20.3 a
Fresh weight debarked (g)	42.2 ± 12.4 a	49.6 ± 12.6 a	49.5 ± 7.8 a	38.6 ± 15.0 a
Dry weight debarked (g)	11.0 ± 4.0 a	12.9 ± 3.2 a	12.8 ± 2.3 a	8.0 ± 3.9 a
Diameter (mm)	9.1 ± 1.4 a	10.4 ± 1.0 a	10.0 ± 1.2 a	9.0 ± 1.7 a

Table 2. Cell wall characteristics of *ccr2 ProSNBE:AtCCR1* poplars. The cell wall residue (CWR, expressed as % of the dry weight) was determined gravimetrically after a sequential extraction. Crystalline cellulose content was determined by the Updegraff method and the mass loss during TFA extraction was used as an estimate of the amount of matrix polysaccharides. Lignin content was determined with the acetyl bromide assay and expressed as % of the CWR. Lignin composition was determined with thioacidolysis. The sum of H, G, and S units is expressed in µmol g^{-1} acetyl bromide lignin. The relative proportions of the different lignin units were calculated based on the total thioacidolysis yield (including the minor nonconventional lignin units). S/G was calculated based on the absolute values for S and G (expressed in µmol g^{-1} acetyl bromide lignin). Different letters represent significant differences at the 0.05 significance level (One-way ANOVA with Tukey's post-hoc test; n = 6 biologically independent samples for wild type, *ccr2 ProSNBE:AtCCR1* lines 3 and 10; n = 8 biologically independent samples for *ccr2 ProSNBE:AtCCR1* line 18). All values are given as means ± standard deviation. n.d., not detected.

	Wild type	***ccr2 ProSNBE:AtCCR1* line 3**	***ccr2 ProSNBE:AtCCR1* line 10**	***ccr2 ProSNBE:AtCCR1* line 18**
CWR (% dry weight)	89.6 ± 0.2 a	89.4 ± 0.4 a	89.2 ± 0.3 a	88.3 ± 0.5 b
Cellulose (% CWR)	42.4 ± 10.4 a	42.3 ± 1.6 a	48.6 ± 7.8 a	48.7 ± 9.5 a
Matrix polysaccharides (% CWR)	39.3 ± 4.0 a	37.2 ± 2.0 a	36.8 ± 2.5 a	36.8 ± 2.2 a
Acetyl bromide lignin (% CWR)	17.7 ± 1.2 a	18.5 ± 1.7 a	18.2 ± 0.9 a	14.5 ± 0.8 b
Thioacidolysis-released monomers				
H+G+S	1.0 ± 0.2 a	0.9 ± 0.2 a	0.9 ± 0.2 a	0.4 ± 0.2 b
%H	0.2 ± 0.1 a	0.2 ± 0.1 a,b	0.1 ± 0.0 a	0.3 ± 0.0 b
%G	26.0 ± 2.0 a	29.3 ± 5.1 a	29.6 ± 4.3 a	29.4 ± 2.6 a
%S	73.8 ± 2.0 a	70.5 ± 5.0 a	70.3 ± 4.3 a	70.3 ± 2.6 a
S/G	2.9 ± 0.3 a	2.5 ± 0.7 a	2.4 ± 0.5 a	2.4 ± 0.3 a
FA-I	n.d.	n.d.	n.d.	0.045 ± 0.035
FA-II	n.d.	n.d.	n.d.	0.018 ± 0.004
CCR marker	n.d.	n.d.	n.d.	0.063 ± 0.048

FIGURES

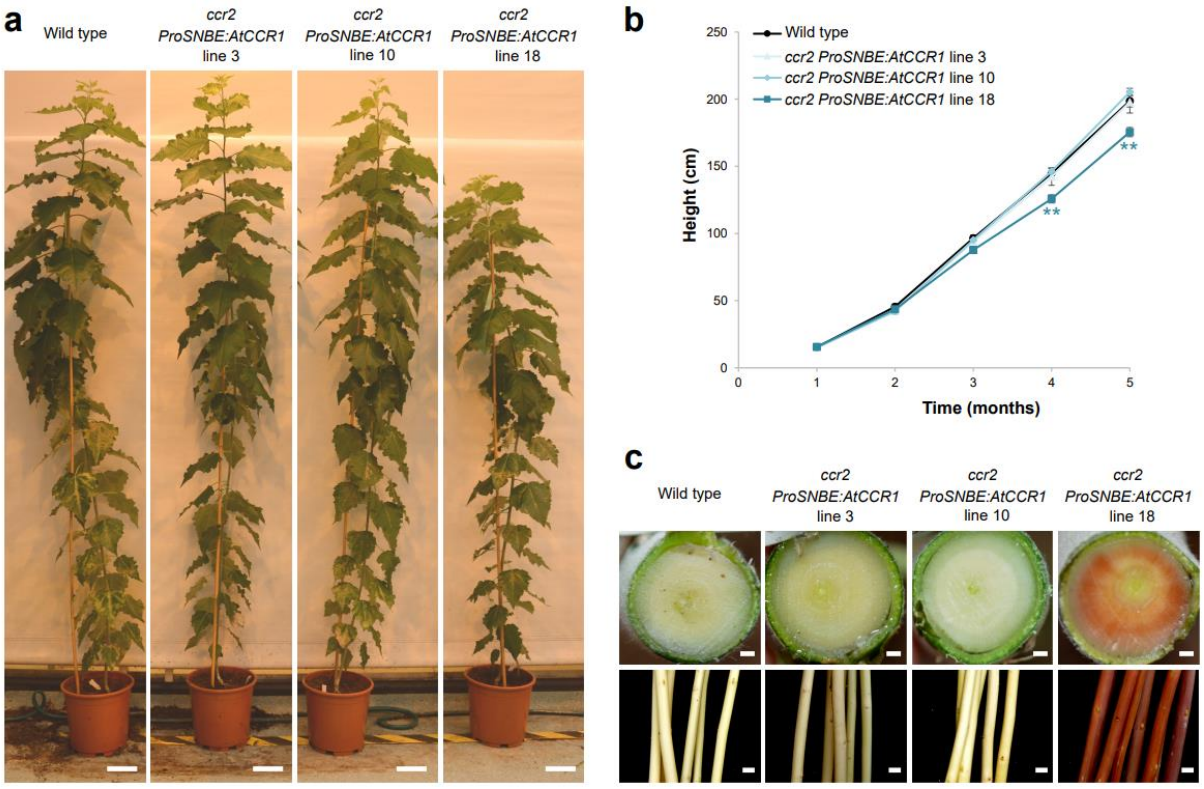

Figure 1. Growth and stem phenotype of *ccr2 ProSNBE:AtCCR1* poplars grown for five months in the greenhouse. (a) Photograph of representative plants. Scale bars = 10 cm. (b) Growth curve. Height was monitored every month for a period of five months. The average height is indicated with a symbol, error bars indicate standard error (n = 6 biologically independent samples for wild type, *ccr2 ProSNBE:AtCCR1* lines 3 and 10; n = 8 biologically independent samples for *ccr2 ProSNBE:AtCCR1* line 18). Differences in growth parameters between the wild type and the transgenic lines were assessed with a One-way ANOVA with Tukey's post-hoc test; $^{**}P < 0.01$. (c) Xylem phenotypic analysis of the cross-section of the stem (upper panels; 10 cm above soil level, scale bars = 1 mm) and debarked stems (lower panels; scale bars = 8 mm).

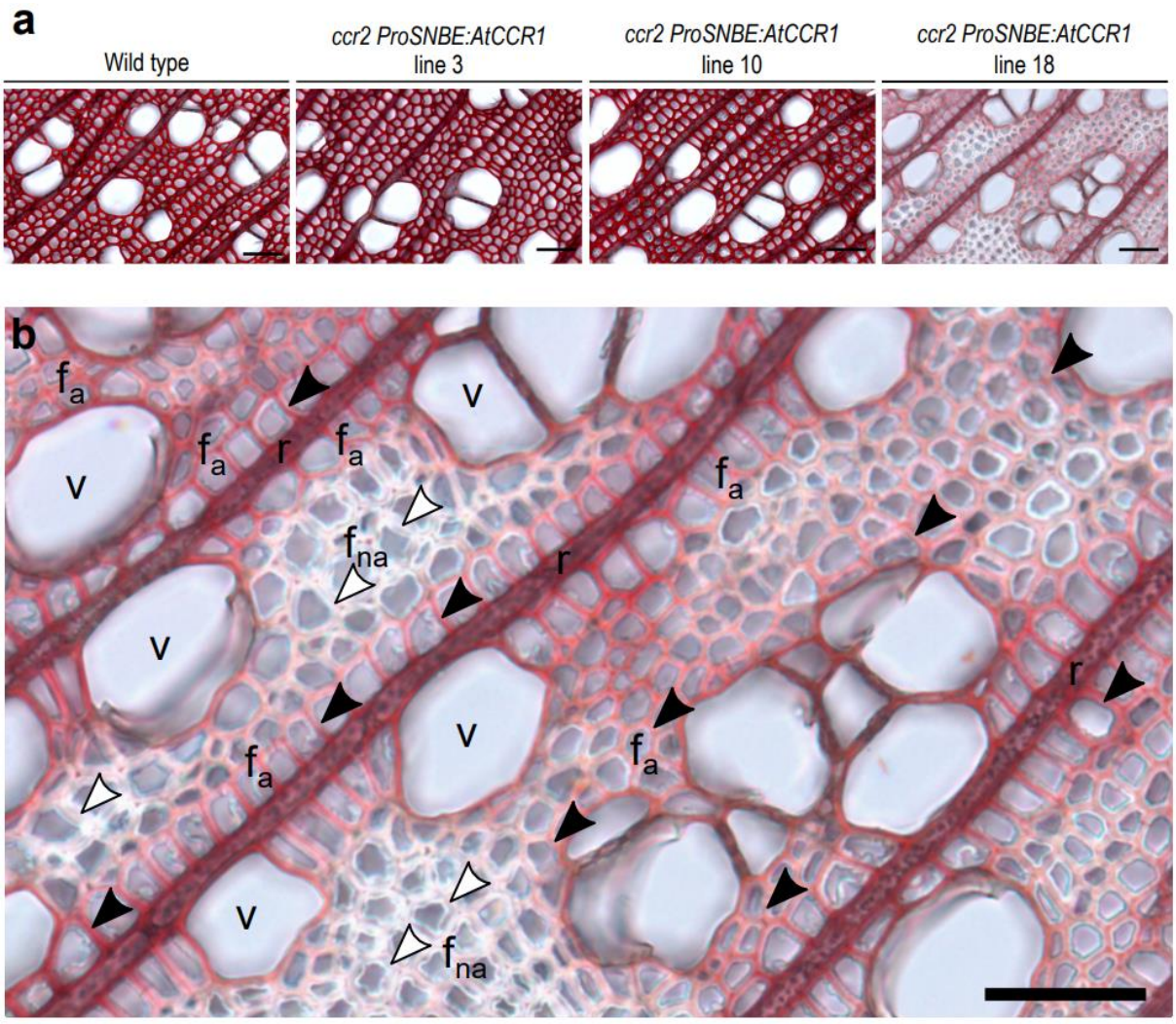

Figure 2. Xylem morphology and lignin deposition in *ccr2 ProSNBE:AtCCR1* poplars. (a) Transverse stem sections of wild type and *ccr2 ProSNBE:AtCCR1* lines visualized with Mäule staining. (b) Enlargement of *ccr2 ProSNBE:AtCCR1* line 18 shown in (a). The cell walls of vessels (v), rays (r), and fibers adjoining vessels and rays (f_a, black arrowheads) showed a more intense coloration compared to the cell walls of non-adjoining fibers located in fiber-rich areas (f_{na}, white arrowheads). Scale bars = 100 µm.

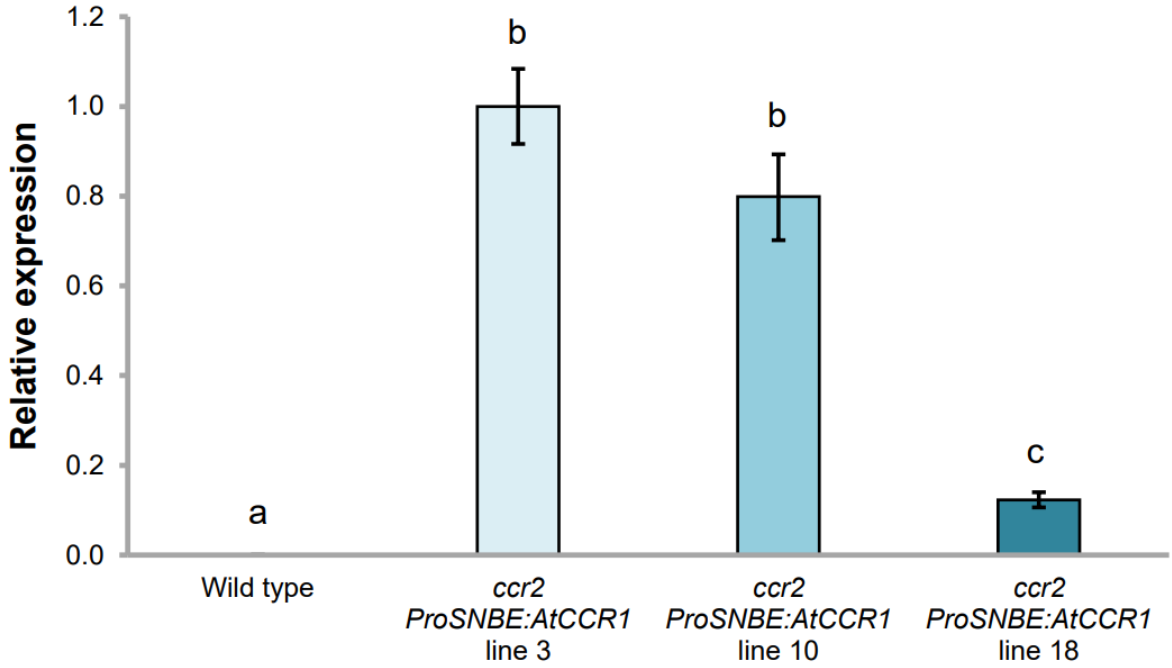

Figure 3. Expression analysis of *AtCCR1* in *ccr2 ProSNBE:AtCCR1* stems as determined via RT-quantitative PCR. Different letters represent significant differences at the 0.001 significance level (One-way ANOVA with Tukey's post-hoc test; n = 3 pooled samples originating from 6 biologically independent samples (pooled by 2) for wild type, *ccr2 ProSNBE:AtCCR1* lines 3 and 10; n = 4 pooled samples originating from 8 biologically independent samples (pooled by 2) for *ccr2 ProSNBE:AtCCR1* line 18). Data represent means ± standard deviation.

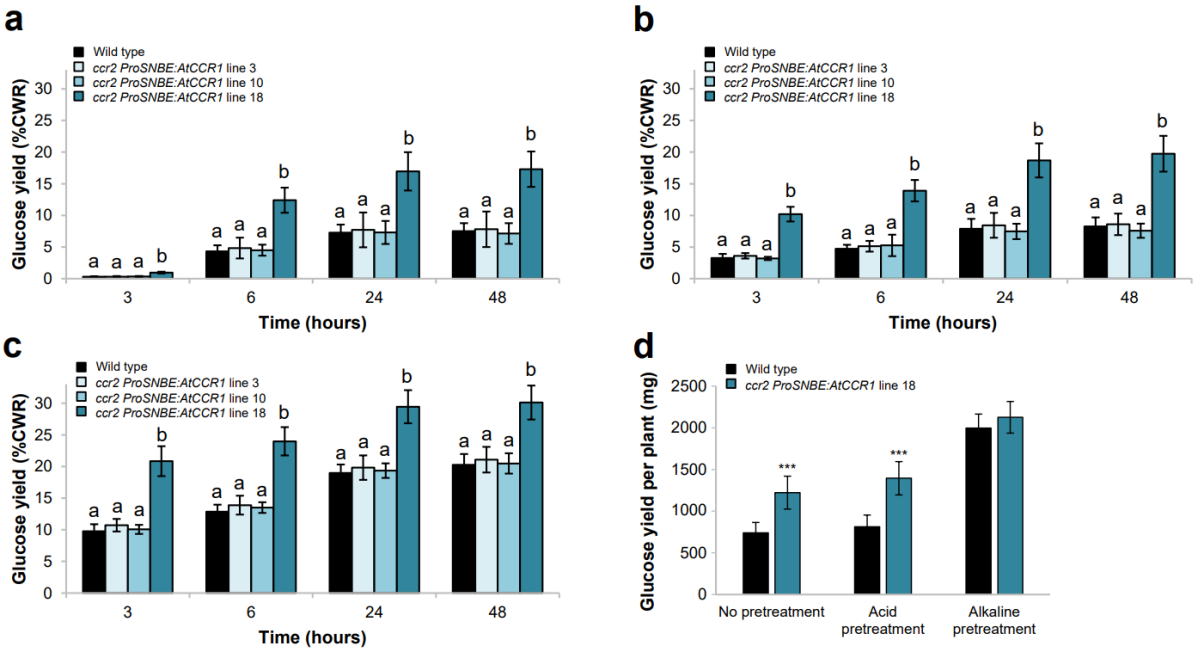

Figure 4. Saccharification assays of *ccr2 ProSNBE:AtCCR1* stems. (a-c) Glucose yield expressed as percentage of cell wall residue (%CWR) for all selected lines after no pretreatment (a), acid pretreatment (b), alkaline pretreatment (c). Different letters represent significant differences at the 0.05 significance level within a specific timepoint (One-way ANOVA with Tukey's post-hoc test; n = 6 biologically independent samples for wild type, *ccr2 ProSNBE:AtCCR1* lines 3 and 10; n = 8 biologically independent samples for *ccr2 ProSNBE:AtCCR1* line 18). (d) Glucose yield after 48h of saccharification expressed on a plant basis for wild type and *ccr2 ProSNBE:AtCCR1* line 18. ****P* < 0.001 (two-tailed Student's *t*-test within a specific pretreatment; n = 6 biologically independent samples for wild type; n = 8 biologically independent samples for *ccr2 ProSNBE:AtCCR1* line 18). Data represent means ± standard deviation.